Role of inhomogeneous broadening in lasing without inversion in ladder systems

Gautam Vemuri*

Department of Physics, Indiana University–Purdue University at Indianapolis (IUPUI), 402 North Blackford Street, Indianapolis, Indiana 46202-3273

Girish S. Agarwal

School of Physics, University of Hyderabad, Hyderabad 500 134, India 6 November 1995

We study the effect of Doppler broadening on the inversionless gain that can be realized in a ladder configuration. The gain is calculated when the strong coherent pump and the weak probe are either copropagating or counterpropagating. The results indicate that the counterpropagating situation is the optimal one for obtaining maximum amplification, since for identical Doppler broadening, the counterpropagating geometry yields higher amplification than the copropagating geometry. The effect of Doppler broadening on electromagnetically induced transparency in the same atomic system is also briefly discussed.

PACS number(s): 42.50.−p, 42.65.Dr

Lasing without population inversion (LWI) has attracted tremendous attention recently. Several theoretical papers and review articles have discussed this phenomenon [1–4], and a few demonstrating experiments have also been reported [5]. While the initial focus of most work was on identifying appropriate atom and field parameters that would yield field amplification without population inversion, later works investigated the quantum statistical properties of radiation from inversionless lasers [6,7]. Since the amount of gain one can realize from inversionless systems is usually quite small, it is important to not only identify the optimal atom and field parameters, but also explore any other issues that may affect the maximal gain one can achieve. In this context, a few groups have suggested replacing the incoherent pump, utilized in most LWI models, with a spectrally colored (partially coherent) pump, which increases the available gain by a factor of 3–4 [8,9]. In attempting to isolate conditions that yield the best gain, little attention has been paid to date to the effect that Doppler broadening has on inversionless gain. Most previous studies on LWI have assumed homogeneously broadened atomic media, and not considered moving atoms [10]. On the other hand, all the experiments reported on LWI so far have been performed in atomic vapors, which are typically accompanied by large Doppler broadening.

Various LWI models have been studied during the past few years, based on two-level, three-level, and four-level atomic systems [1–4,11–13]. In this paper, we focus on a specific three-level ladder system, shown in Fig. 1, and determine the influence of Doppler broadening on the inversionless gain [14]. The energy-level scheme of Fig. 1 is relevant to the ^{138}Ba [8] or the ^{87}Rb atom, where the $|1\rangle \leftrightarrow |3\rangle$ transition is dipole forbidden. Levels $|1\rangle$ and $|2\rangle$ decay to the next lower-lying levels and have radiative widths of $2\gamma_1$ and $2\gamma_2$. The lower transition, at atomic frequency ω_{23}, is driven by a strong, coherent field, at a frequency ω_2. The $|1\rangle \leftrightarrow |2\rangle$ transition, at an atomic frequency ω_{12}, is the lasing transition, on which an incoherent pump transfers population to

the upper lasing state, at a rate Λ. A weak probe, of frequency ω_1, is scanned across this transition, and its gain or absorption monitored. By choosing the strength of the coherent field, its detuning from the relevant transition, and the rate of incoherent pumping, suitably, one can realize amplification of the probe when the $|1\rangle \leftrightarrow |2\rangle$ transition is uninverted [8]. We first outline our discussion for a stationary atom, and then point out the necessary changes to modify the model and include Doppler effects. The semiclassical Hamiltonian that describes our atom-field system, in a frame rotating at the fast optical frequencies, is given by

$$H = \hbar\{(\Delta_1 + \Delta_2)|1\rangle\langle 1| + \Delta_2|2\rangle\langle 2|$$
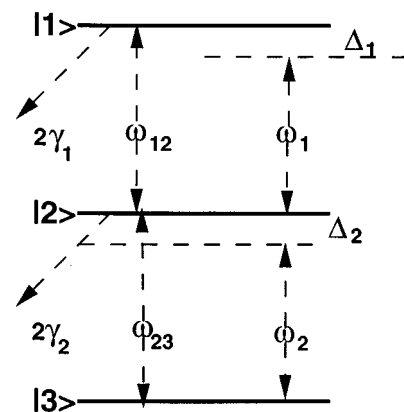$$- [g|1\rangle\langle 2| + G_2|2\rangle\langle 3| + \text{H.c.}]\}, \qquad (1)$$

FIG. 1. Schematic representation of a three-level ladder system with ground state $|3\rangle$ and two excited states $|1\rangle$ and $|2\rangle$. The spontaneous decay rates from $|1\rangle$ to $|2\rangle$ and $|2\rangle$ to $|3\rangle$ are $2\gamma_1$ and $2\gamma_2$, respectively. The transition from $|1\rangle$ to $|3\rangle$ is not allowed. ω_{12} and ω_{23} are the resonance frequencies of the upper and lower transitions respectively, and ω_1 and ω_2 are the frequencies of the probe and coherent pump fields, respectively. Incoherent pumps on $|1\rangle \leftrightarrow |2\rangle$ are not shown.

---

*Electronic address: gvemuri@indyvax.iupui.edu

where $\Delta_1=\omega_{12}-\omega_1$, $\Delta_2=\omega_{23}-\omega_2$, and G_2 is the Rabi frequency of the strong coherent pump on the lower transition, given by

$$G_2=\frac{\vec{d}_{23}\cdot\vec{\epsilon}_2}{\hbar}. \qquad (2)$$

In Eq. (2), d_{23} is the dipole moment matrix element associated with the $|2\rangle\leftrightarrow|3\rangle$ transition and ϵ_2 is the amplitude of the coherent pump field. In Eq. (1), g is the Rabi frequency of the weak probe on the upper transition. It is straightforward to derive the time evolution of the relevant density matrix elements, from the Hamiltonian, which we list below, along with the contribution of the radiative decay terms, and the incoherent pump rate

$$\dot{\rho}_{11}=-2\gamma_1\rho_{11}+ig\rho_{21}-ig^*\rho_{12}-2\Lambda(\rho_{11}-\rho_{22}), \quad (3a)$$

$$\dot{\rho}_{12}=-(\gamma_1+\gamma_2+i\Delta_1)\rho_{12}+ig(\rho_{22}-\rho_{11})-iG_2^*\rho_{13}$$
$$-2\Lambda\rho_{12}, \qquad (3b)$$

$$\dot{\rho}_{13}=-(\gamma_1+i\Delta_1+i\Delta_2)\rho_{13}+ig\rho_{23}-iG_2\rho_{12}-\Lambda\rho_{13}, \qquad (3c)$$

$$\dot{\rho}_{22}=2\gamma_1\rho_{11}-2\gamma_2\rho_{22}-ig\rho_{21}+ig^*\rho_{12}+iG_2\rho_{32}-iG_2^*\rho_{23}$$
$$+2\Lambda(\rho_{11}-\rho_{22}), \qquad (3d)$$

$$\dot{\rho}_{23}=-(\gamma_2+i\Delta_2)\rho_{23}+ig^*\rho_{13}+iG_2(\rho_{33}-\rho_{22})-\Lambda\rho_{23}, \qquad (3e)$$

$$\dot{\rho}_{33}=2\gamma_2\rho_{22}-iG_2\rho_{32}+iG_2^*\rho_{23}. \qquad (3f)$$

The gain G is given by calculation of the density matrix element ρ_{12}, and explicitly is

$$G=-\mathrm{Im}\left(\frac{\rho_{12}\gamma_1}{g}\right), \qquad (4)$$

where G is in units of the weak-field resonant absorptivity [8]. By treating the weak probe perturbatively to first order, one can solve for ρ_{12} analytically, which yields

$$\rho_{12}=\frac{(\gamma_1+i\Delta_1+i\Delta_2+\Lambda)ig(\rho_{22}^0-\rho_{11}^0)+G_2^*g\rho_{23}^0}{(\gamma_1+\gamma_2+i\Delta_1+2\Lambda)(\gamma_1+i\Delta_1+i\Delta_2+\Lambda)+|G_2|^2}, \qquad (5)$$

where ρ_{11}^0, ρ_{22}^0, and ρ_{23}^0 are obtained from the zeroth-order solutions of the density matrix equations in Eq. (3), and are

$$\rho_{11}^0=\frac{k\Lambda}{3k\Lambda+2k\gamma_1+2\Lambda\gamma_2+2\gamma_1\gamma_2}, \qquad (6a)$$

$$\rho_{22}^0=\frac{\rho_{11}^0(\Lambda+\gamma_1)}{\Lambda}, \qquad (6b)$$

$$\rho_{23}^0=\frac{iG_2(1-\rho_{11}^0-2\rho_{22}^0)}{\gamma_2+i\Delta_2+\Lambda}, \qquad (6c)$$

where

$$k=\frac{2|G_2|^2(\gamma_2+\Lambda)}{(\gamma_2+\Lambda)^2+\Delta_2^2}. \qquad (7)$$

As already stated, the calculation of the gain outlined above is valid for a stationary atom. We now consider atomic motion and the resulting gain when Doppler effects are included. For a single atom, moving with a velocity v along the z axis, the probe frequency $\omega_1(v)$, as seen by the atom, is given by

$$\omega_1(v)=\omega_1(1\pm v/c), \qquad (8a)$$

where the negative (positive) sign corresponds to copropagating atom and probe (counterpropagating atom and probe). Similarly, the frequency of the coherent pump $\omega_2(v)$, as seen by the atom is

$$\omega_2(v)=\omega_2(1\pm v/c). \qquad (8b)$$

We denote by $\delta_1(v)$ and $\delta_2(v)$, the detunings of the probe and coherent pump from their respective transitions, as seen by the moving atom. This implies that $\delta_1(v)=-\omega_1(v)+\omega_{12}$ and $\delta_2(v)=-\omega_2(v)+\omega_{23}$. We can rewrite $\delta_2(v)$ in terms of $\delta_1(v)$ and the stationary atom parameters as

$$\delta_2(v)=\Delta_2\pm\frac{\omega_2}{\omega_1}[\delta_1(v)-\Delta_1],$$

$$\delta_1(v)=\omega_{12}-\omega_1(1\pm v/c)\equiv\Delta_1\mp\omega_1 v/c. \qquad (9)$$

To further simplify the analysis, we set $\omega_1=\omega_2$ in Eq. (9). Assuming a Maxwell-Boltzmann distribution for the atomic velocities, we adopt a probability distribution function for $\delta_1(v)$, which is given by

$$\rho(\delta_1)=\frac{1}{\sqrt{2\pi D^2}}e^{-(\delta_1-\Delta_1)^2/2D^2}. \qquad (10)$$

The inversionless gain, averaged over the Doppler distribution, is obtained from

$$G=-\mathrm{Im}\int_{-\infty}^{\infty}\rho_{12}(\delta_1)\rho(\delta_1)d\delta_1. \qquad (11)$$

To obtain the probe response that is averaged over the Doppler distribution, we replace Δ_1 in Eq. (3) by $\delta_1(v)$, which has a probability distribution of the form in Eq. (10). Further, we replace Δ_2 in Eq. (3) by $\delta_2(v)$, which is given in terms of $\delta_1(v)$, Δ_1, and Δ_2 by Eq. (9).

In the results that we describe next, we have numerically solved for the inversionless gain, as a function of Δ_1, for different values of the Doppler widths. All rates are in units of γ_1. The parameter values are $\gamma_2=5.45$, $G_2=14.3$, $\Delta_2=25.1$, and $\Lambda=1.7$ [except for Fig. 3(b)]. The numerical algorithm consists of calculating ρ_{12} in Eq. (5), in the presence of Doppler broadening. For a given D and Δ_1, we generate a distribution of δ_1 via the use of Eq. (10). The resulting values of δ_1 were centered at the selected value of Δ_1, and the typical distribution was over an interval 100 times the Doppler width. This interval range was found to be sufficient for producing consistent and accurate results. For each value of δ_1, we determined δ_2 from Eq. (9). Then, for each δ_1 and
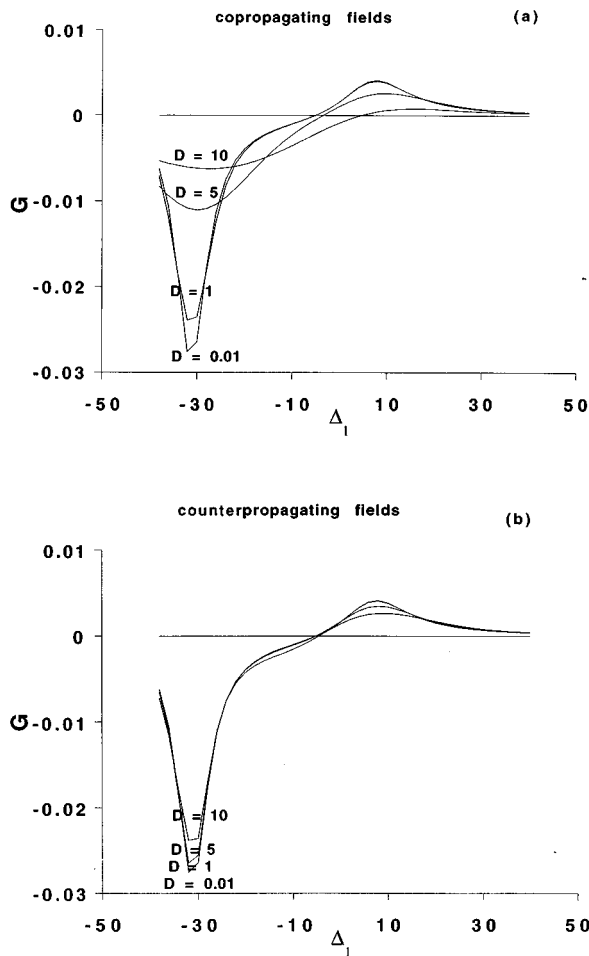
FIG. 2. (a) Probe response as a function of Δ_1 for copropagating pump and probe fields. The four curves correspond to D of 0.01, 1.0, 5.0, and 10. (b) Probe response as a function of Δ_1 for counterpropagating pump and probe fields. The four curves correspond to D of 0.01, 1.0, 5.0, and 10. Note that curves for $D=0.01$ and $D=1$ are indistinguishable.
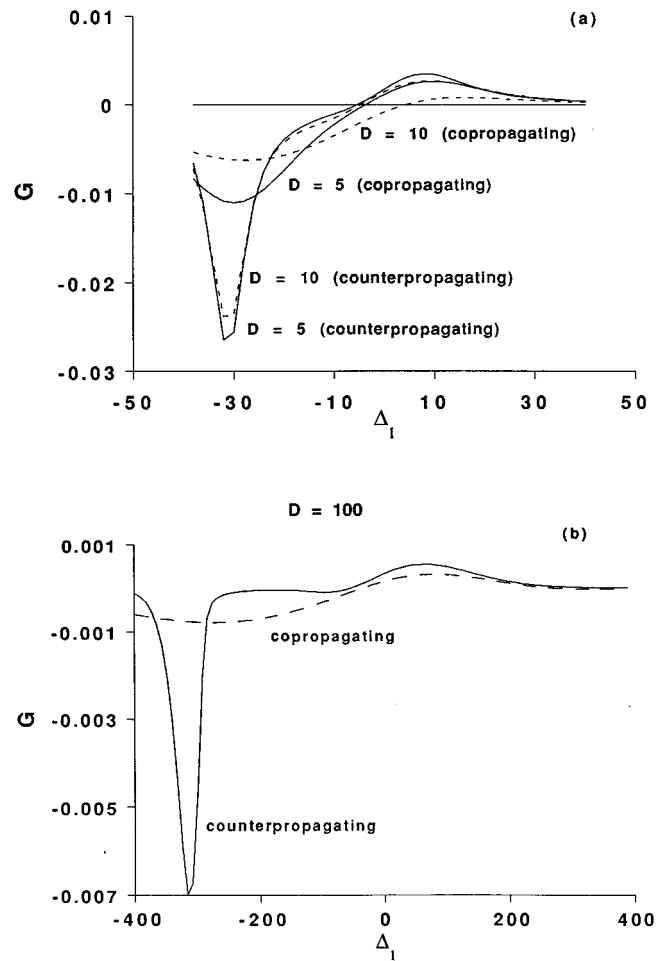
FIG. 3. (a) Probe response as a function of Δ_1 for copropagating and counterpropagating pump and probe fields, for D of 5 (solid line) and 10 (dashed line). (b) Probe response as a function of Δ_1 for copropagating (dashed line) and counterpropagating (solid line) pump and probe fields, for $D=100$, $G_2=143$, $\Delta_2=251$, $\Lambda=1.7$, and $\gamma_2=5.45$.

δ_2, Eq. (5) was used to calculate ρ_{12}. To determine the Doppler averaged signal as given by Eq. (11), we simply summed the signal from the contributions due to the various values of δ_1, distributed in accordance with Eq. (10).

The range of Doppler widths we studied was from 0.01 to a maximum of 10. Note that numerical reasons prevent us from studying $D=0$ [as seen from Eq. (10)], and so we use $D=0.01$ as representative of zero Doppler width. This assertion has been carefully checked by comparing the gain profile for a stationary atom with one where the Doppler width is 0.01 and ensuring that the results are identical. Such small values of Doppler broadening are also encountered in vapor cell traps. In rubidium vapor traps, at typical temperatures of 150–250 μK, one can obtain atomic velocities of 15 cm/s, which would correspond to Doppler widths of 200 kHz. A natural linewidth of 5.9 MHz would then imply a D of 0.03. D values of 0.1–1 are typical of the residual broadening one encounters in atomic-beam experiments, where one can arrange the two fields to be perpendicular to the atomic beam.

In Fig. 2(a) is shown the probe response, averaged over the Doppler broadening, when the pump and probe fields are copropagating. The four curves correspond to Doppler widths of 0.01, 1, 5, and 10. The first curve corresponds almost identically to the response from a stationary atom, validating our choice of $D=0.01$ as being close to zero Doppler width. It is quite clear from this figure that as the Doppler width increases, there is a rapid decrease in the maximum gain that one can realize in this atomic system. Figure 2(b) shows the results when the pump and probe fields are counterpropagating. We find that the effect of Doppler broadening is much less severe in this geometry, and that even for Doppler widths that are 10 times the natural width, there is very little reduction in gain from the stationary atom case. This indicates that the counterpropagating geometry is the preferred one for realizing optimal gain in a three-level ladder system. To further elaborate on this point, we next compare the gain for copropagating and counterpropagating geometries, for identical Doppler widths. Specifically, the gain in the copropagating geometry decreases much faster than in the counterpropagating geometry, as seen in Fig. 3(a). Clearly, the difference in the gain profiles for a Doppler width of 10 is quite pronounced between the two different field configurations. Since typical vapor cells produce Doppler widths of 100 times the radiative widths, in Fig. 3(b) we
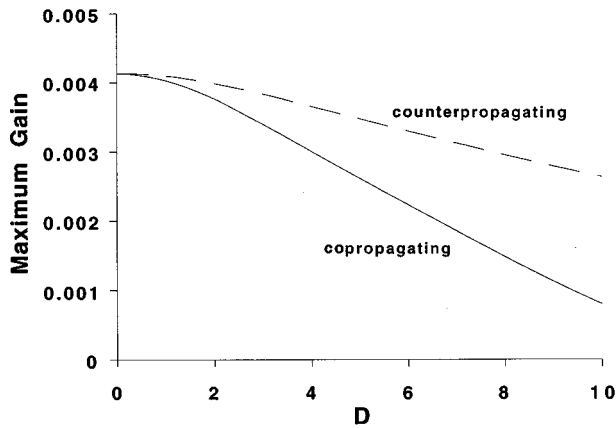
FIG. 4. Maximum gain vs Doppler width D for the two geometries, for parameters of Fig. 3(a).

FIG. 5. Probe response as a function of Δ_1, for the two cases of copropagating and counterpropagating pump and probe fields. The three curves correspond to D of 0.01, 1.0, and 10 in (a) and (b). Other parameters are $\Delta_2 = \Lambda = 0$, $G_2 = 14.3$, and $\gamma_2 = 5.45$.

show a comparison of the probe absorption spectrum for co-propagating and counterpropagating geometries when $D = 100$. We have now chosen larger values of G_2 and Δ_2, to clearly reveal the differences between the two geometries. It is apparent that the distinction between maximum absorption and gain for the copropagating geometry is not well resolved, since they are both close to zero. On the other hand, the counterpropagating geometry again provides higher gain, and a much greater distinction between the absorption levels and the gain levels, indicating that the counterpropagating geometry should be the preferred one.

Since the maximum gain varies with the Doppler width, in Fig. 4 we show the maximum gain as a function of the Doppler width. The value of Δ_1, at which the maximum gain appears, shifts with change in the Doppler width. This is to be expected, since a Doppler width can be considered as equivalent to a value of Δ_2 different from that for a stationary atom (25.1 in our case), and we know that different values of Δ_2 produce maximum gain at different probe detunings. However, in Fig. 4, we have plotted the *maximum* gain, as a function of D, and one can see that the gain drops off much more sharply for copropagating fields than it does for counterpropagating fields.

The difference in gain levels is quite dramatic for large inhomogeneous broadening, i.e., in the regime where the Doppler width is comparable to the Rabi frequency of the pump. In this regime, the usual argument for Doppler-free two-photon spectroscopy will imply that the gain should be substantially higher for counterpropagating fields than for copropagating fields. Figure 4 shows the inversionless gain for these two geometries, and it is clear that the differences in gain become more pronounced as D increases.

Since we are discussing inversionless amplification, it is worth saying a word about the populations in levels $|1\rangle$ and $|2\rangle$. The populations that one is concerned with are the occupation probabilities in the absence of the probe field, i.e., ρ_{11}^0 and ρ_{22}^0, as given by Eqs. (6) and (7). It is clear from these expressions that the population difference, $\rho_{11}^0 - \rho_{22}^0$ is negative, implying that the atom is always uninverted. Even in the presence of Doppler broadening, it is easy to show from Eqs. (6) and (7) that the atoms are inversionless.

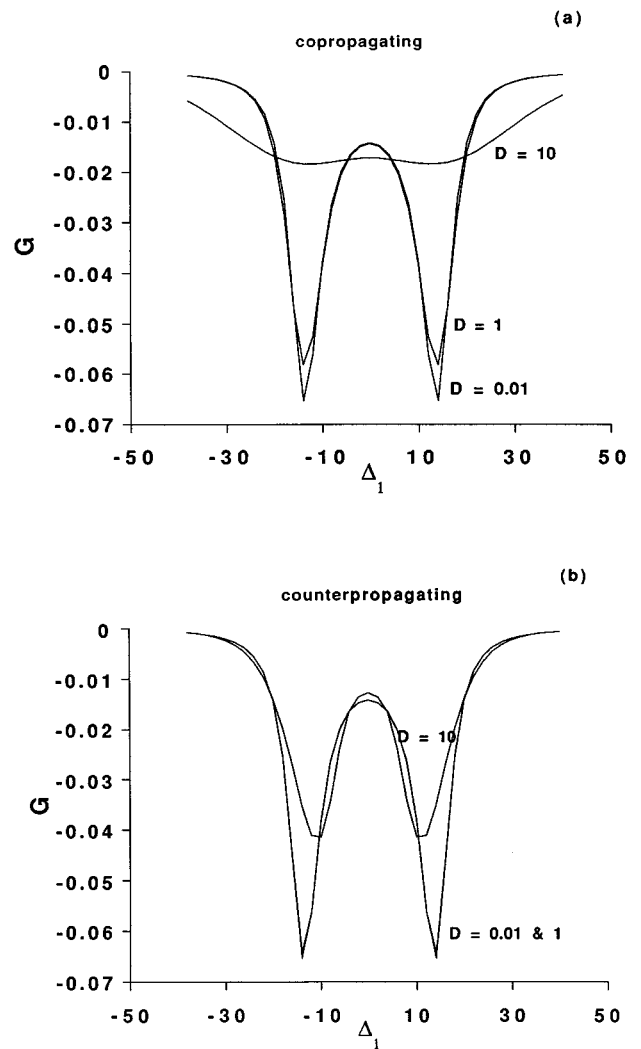It is quite easy to investigate the effect of Doppler broad-

ening on electromagnetic field induced transparency (EIT) in our system [15,16]. We have done this by setting $\Lambda = 0$ and studied the case when $\Delta_2 = 0$. In Fig. 5(a) is the probe response for copropagating fields. We see clear evidence of the two Autler-Townes peaks at the Rabi frequencies of the coherent pump. With increasing Doppler widths, one sees a reduction in the signal. Just as in the case of LWI, even for EIT, the effect of Doppler broadening is far less when the pump and probe fields are counterpropagating, as shown in Fig. 5(b).

In summary, we have studied the effect of inhomogeneous broadening on the inversionless gain in a three-level ladder system. By comparing the effects of Doppler broadening, when the pump and probe are copropagating and counterpropagating, we have identified that the optimal geometry is for the pump and probe to be counterpropagating. In particular, our results indicate that as the Doppler width increases, the effect on the gain is severe when the two fields are co-

propagating, and much smaller when the fields are counter-propagating. The decrease in gain with Doppler width is much faster for the copropagating geometry than for the counterpropagating geometry. We have also investigated the effect of Doppler broadening on EIT and the conclusions are identical to those for LWI. It should be mentioned here that these results, while true for a ladder system, may not necessarily hold true for other energy-level configurations.

[1] O. Kochaorvskaya, Phys. Rep. **219**, 175 (1992).

[2] M. O. Scully, Phys. Rep. **219**, 219 (1992).

[3] P. Mandel, Contemp. Phys. **34**, 235 (1994).

[4] See special issue of Quantum Opt. **6**, 201–389 (1994).

[5] J. Y. Gao *et al.*, Opt. Commun. **93**, 323 (1992); A. Nottelmann *et al.*, Phys. Rev. Lett. **70**, 1783 (1993); W. E. van der Veer *et al.*, *ibid.* **60**, 3243 (1993); E. S. Fry *et al.*, *ibid.* **70**, 3235 (1993).

[6] G. S. Agarwal, Phys. Rev. Lett. **67**, 980 (1991).

[7] K. Gheri and D. F. Walls, Phys. Rev. Lett. **68**, 3428 (1992); Phys. Rev. A **45**, 6675 (1992).

[8] G. S. Agarwal, G. Vemuri, and T. W. Mossberg, Phys. Rev. A **48**, R4055 (1993); G. Vemuri and D. M. Wood, *ibid.* **50**, 747 (1994); G. Vemuri, Quantum Opt. **6**, 305 (1994).

[9] K. K. Meduri, P. B. Sellin, G. A. Wilson, and T. W. Mossberg, Quantum Opt. **6**, 287 (1994).

[10] D. Z. Wang and J. Y. Gao, Phys. Rev. A **52**, 3201 (1995), have calculated Doppler broadening effects in four-level systems.

[11] A. Lezama, Y. Zhu, M. Kanskar, and T. W. Mossberg, Phys. Rev. A **41**, 1576 (1990).

[12] A. Imamoglu, J. E. Field, and S. E. Harris, Phys. Rev. Lett. **66**, 1154 (1991); G. B. Prasad and G. S. Agarwal, Opt. Commun. **86**, 409 (1991); Y. Zhu, Phys. Rev. A **45**, R6149 (1992).

[13] H. M. Doss *et al.*, Opt. Commun. **95**, 57 (1992). These authors also include Doppler broadening in the four-level model.

[14] Doppler effects in V and Λ configurations, in the context of LWI, have been reported by A. Karawajczyk and J. Zakrzewski, Phys. Rev. A **51**, 830 (1995).

[15] S. E. Harris, J. E. Field, and A. Imamoglu, Phys. Rev. Lett. **64**, 1107 (1990); S. P. Tewari and G. S. Agarwal, *ibid.* **56**, 1811 (1986).

[16] The effects of Doppler broadening were included in the (a) earlier calculations on nonlinear generation by Harris *et al.* (Ref. [15]) and by S. P. Tewari and G. S. Agarwal, Phys. Rev. Lett. **66**, 1797 (1991); (b) J. Gea-Banacloche, Y. Li, S. Jin, and M. Xiao, Phys. Rev. A **51**, 576 (1995); M. Xiao, Y. Li, S. Jin, and J. Gea-Banacloche, Phys. Rev. Lett. **74**, 666 (1995).